Multiple Slip Effects on a Rotating Second-Grade Fluid Model Over a Stretching Sheet Under the Influence of Dufour and Soret

Dr.S.Aiswarya[1*], G.Vidhya[2]

[1] *Department of Mathematics, PSGR Krishnammal College for Women, Coimbatore, India*
[2] *Department of Mathematics, PSGR Krishnammal College for Women, Coimbatore, India*
[1]*aishwaryas@psgrkcw.ac.in* , [2]*vidhya1701g@gmail.com*

Abstract: *The interplay of rotation, multiple slip effects, the Dufour effect, and second-grade fluid is crucial in advanced applications such as aerospace systems, biomedical devices, chemical processing, geophysics, and micro- and nanotechnology. Hence this study investigates the impact of multiple slip effects on the rotating three-dimensional viscoelastic fluid flow over an expandable heated surface, incorporating the influences of Soret and Dufour effects. The analysis employs the second-grade fluid model to capture viscoelasticity, with the Coriolis force included in the governing equations due to the rotational frame assumption. Using similarity transformations, the equations are non-dimensionalized and solved numerically via the bvp5c solver in MATLAB. The observed results show that, slip effects cause magnified velocity, temperature, and concentration, making the model extremely useful in microfluidic transport, thermal management, and surface-engineered flow systems. Meanwhile, the intricate interaction of rotational dynamics and fluid elasticity broadens its application to polymer manufacturing, biological flows, and rotating devices. Overall, these findings provide useful insights for optimizing advanced non-Newtonian fluid technologies in a variety of engineering applications.*

Keywords: Second grade model, Rotation, Dufour, Soret, Multiple slips.

Nomenclature

Re_x	Local Reynolds number
u, v, w	Velocity components along x, y, z
T	Temperature
C	Concentration
B_0	Magnetic flux density
M	Magnetic field parameter
Pr	Prandtl number
Sc	Schmidt number
Sr	Soret number
Df	Dufour number
Ec	Eckert number
D	Mass diffusivity
$\boldsymbol{V}$	Velocity vector
$\boldsymbol{r}$	Position vector
p	Pressure
K	Elasticity coefficient
J	Current density
$\boldsymbol{B}$	Magnetic field vector

*Corresponding Author

$\boldsymbol{I}$	Identity tensor
$\boldsymbol{A_1}, \boldsymbol{A_2}$	First and Second Rivlin-Ericksen tensors
C_f	Skin friction coefficient
Nu_x	Local Nusselt number
Sh_x	Local Sherwood number
q_w	Heat flux at the wall
j_w	Mass flux at the wall
k_T	Thermophoretic diffusion coefficient
T_s	Surface temperature
C_s	Surface concentration
T_∞	Ambient temperature
C_∞	Ambient concentration
T_m	Mean temperature
c_p	Specific heat capacity
c_s	Specific heat at saturation

Greek symbols

γ	Velocity slip parameter
α	Thermal slip parameter
β	Concentration slip parameter
ν	Kinematic viscosity
ρ	Fluid density
μ	Dynamic viscosity
ξ	Similarity variable
$\theta(\xi)$	Dimensionless temperature
$\phi(\xi)$	Dimensionless concentration
Ω	Angular velocity
λ	Rotation parameter (Ω/a)
α_1	Material fluid parameter
σ	Electrical conductivity
κ	Thermal conductivity
∇	Gradient operator
∇^2	Laplacian operator
$\mathcal{T}$	Stress tensor
$\mathcal{T}_{zx}, \mathcal{T}_{zy}$	Stress components along x and y directions

1. INTRODUCTION

In classical fluid mechanics, the no-slip condition explains how a viscous fluid behaves near a solid boundary. However, experimental studies and modern applications shows that this assumption does not hold in many situations, particularly for non-Newtonian fluids, micro and nanoscale transport, and flows over hydrophobic or engineered surfaces. In such cases, slip effect plays a significant role, as they modify the momentum and thermal boundary layers, reduce wall shear, and influence heat and mass transfer performance. Accounting for slip is therefore essential for achieving realistic predictions of flow behavior in polymer processing, biological fluids, microfluidic devices, and high-precision thermal systems. Thereby, contemporary models increasingly incorporate single or multiple slip conditions to accurately represent interfacial behavior and improve the physical relevance of theoretical analysis.

Non-Newtonian fluids are a prominent field of study in fluid dynamics. It differs from Newtonian fluids in that their viscosity varies based on the rate of deformation, rather than being directly proportionate. The versatility of non-Newtonian fluids makes them crucial for numerous applications such as pharmaceutical formulations, polymer processing, slurry transport, wastewater treatment, and coatings because to their impact on energy and species transfer. Beyond industrial uses, non-Newtonian fluids play a critical part in physiological processes such as blood flow as well as geophysical and oil exploration. Fluids are classified as viscoelastic (e.g., polymer melts and hydrogels), shear-thickening (e.g., water and honey), or shear-thinning (e.g., paint and yogurt). Each of these groups exhibits distinct flow characteristics under varied circumstances. A thorough comprehension of these characteristics is essential for improving flow management tactics and honing analytical methods. Non-Newtonian fluids are modeled using a variety of correlation techniques to describe their viscous characteristics, particularly when flow behavior adjusts to shifting shear stress circumstances. Lavrov [1] investigated how non-Newtonian fluids move over fractured media, highlighting the difficulties in precisely simulating their flow properties. In their study of mixed convection processes, Khan et al. [2] concentrated on entropy generation and activation energy. Alharbi et al. [3] looked into Coriolis forces and viscous dissipation's effects on three-dimensional non-Newtonian fluid flow highlight how crucial rotational motion is. In their analysis of co-extrusion processes in rectangular ducts, Hammer et al. [4] showed how rheology and flow behavior are related. Furthermore, Hashim et al. [5] investigated coupled mass and energy transport in non-Newtonian nanofluid flows, providing insight into the mechanisms behind solute and heat transfer. In their study of mixed convection in magnetized non-Newtonian fluids, Rehman et al. [6] took into account how heat generation is impacted by viscous dissipation.

Viscoelastic fluids are distinguished from other non-Newtonian fluids by their unique combination of viscous and elastic properties. They are particularly pertinent in fields including polymer processing, biomedical applications, and energy systems because of their unique nature. In a provocative research, Ali et al. [7] showed how magnetic fields affect flow stability by examining the Hartmann boundary layer peristaltically flowing viscoelastic fluids. Electrical conductivity and boundary conditions in magnetized non-Newtonian nanofluid peristaltic transport were investigated by Vaidya et al. [8]. To illustrate the complicated relationship between electromagnetic forces and fluid movement, Akram et al. [9] investigated the effects of Hall potential and ion slip on dual-phase radiating non-Newtonian nanofluid motion. Fakhar et al. [10] studied entropy formation in Walters-B viscoelastic fluids while controlling for external magnetic field influences and frictional heating.

Second-grade fluids, a type of non-Newtonian fluids, have drew considerable focus from academics owing to its ability to imitate real-world occurrences including geothermal processes and polymeric flows. Bilal et al. [11] examined the hydromagnetic flow of a second-grade fluid around an inclined permeable cylinder, focusing on Joule heating and radiative heat transfer. Hosseinzadeh et al. [12] expanded on this investigation by investigating MHD second-grade viscoelastic flow of nanofluid under varied temperature conditions. Mustafa et al. [13] studied the convective behavior of second-grade fluids across an upright substrate subjected to heating to assess the impact of heat flow changes.

Fluid flow over stretched sheets has gained considerable amount of attention due to its vital uses in wire drawing, polymer extrusion, and aerodynamic boundary layers, among other fields. The investigation of viscous flow across a nonlinearly extending sheet in early research, like that done by Vajravelu [14], revealed differences in heat transmission within boundary layers. Velocity slip and convective heating effects were included in Alrehili's [15] analysis of viscoelastic nanofluid flow over an extensible surface. Eid and Mabood [16] studied the MHD flow of second-grade viscoelastic non-Newtonian nanofluids over curved stretched sheets, accounting for electromagnetic spectrum and heat transmission effects. Maxwell (UCM) fluid motion over a permeable extended sheet was examined by Abdelsalam et al. [17], who concentrated on fluid elasticity and how it affects heat transfer. Rehman et al. [18] investigated non-Fourier heat conduction methods using Cattaneo-Christov thermal flux and Soret-Dufour processes in viscoelastic fluid flow across a stretched sheet. Zeb et al. [19] looked at how electromagnetic radiation and MHD affected viscoelastic UCM fluids moving through porous medium during slip.

The main focus of research on stretching sheet problems is boundary layer behavior close to moving surfaces; rotation has a big influence on industrial, geophysical, and astronomical flows. Bilal et al. [20] investigated the interactions between magnetic fields and suspended particles in highly elastic dusty fluids in a rotating frame. Khan et al. [21] investigated Newtonian heating in a revolving Couette flow and assessed energy efficiency by entropy generation analysis. In a rotating system, Akbar and Mustafa [22] explored coupled heat and mass transmission in viscoelastic fluids, revealing complicated thermal properties. Hayat et al. [23] investigated the Soret-Dufour effects in MHD rotating viscoelastic fluid flow.

Heat and mass transmission are fundamentally influenced by the thermophoresis and diffusion-thermo effects. These effects in magnetoconvection over an inclined plate with heat source/sink influences were investigated by Mondal et al. [24]. Their influence on energy transport was demonstrated by Rashidi et al.'s investigation of their function in viscoelastic MHD flow [25]. The effects of Dufour and thermal diffusion on time-dependent free convection transport were investigated by Hasanuzzaman et al. [26]. Harikrushna et al. [27] analyzed these effects in MHD Maxwell nanofluid flow, emphasizing their significance in microfluidic transport. In their study of bioconvective Maxwell fluid energy transmission, Ahmed et al. [28] shown how thermal diffusion interacts with the fluid. Sudarmozhi et al. [29] studied viscoelastic fluid flow in porous media, considering activation energy influences on heat and mass transport. Sreedevi et al. [30] analyzed Soret-Dufour effects in MHD flow over a permeable stretching sheet, demonstrating alterations in boundary layer behavior.

Boundary layer behavior and thermal transport are greatly affected by multiple slip conditions. Hasanuzzaman et al. [31] provided insights into the role of heat generation and radiation in MHD convective transport over a vertical permeable sheet, where boundary layer behavior was influenced by multiple slip conditions. The impact of multiple slips on the bioconvective MHD flow of non-Newtonian fluids was examined by Gautam et al. [32], demonstrating increase in the effectiveness of heat transmission. Abbas et al. [33] analyzed Jeffrey fluid flow past a stretching Riga curved surface, incorporating Soret-Dufour effects and their influence on energy dissipation. This study was extended by Chamkha et al. [34] to unstable mixed convection MHD flow, taking slip boundary conditions and chemical interactions into consideration. In order to highlight the importance of electrically conducting fluids in improving convective heat transfer, Asmat et al. [35] investigated how these fluids behaved under various slip and radiation impacts. Sudarmozhi et al. [36] studied viscoelastic fluid flow over a flat plate, considering boundary slip and suction effects, contributing to advancements in thermal management strategies.

A detailed examination of the existing literature highlights several important gaps requiring further exploration. This study addresses these gaps by incorporating the Dufour effect and additional slip conditions into the flow model of Akbar and Mustafa [22]. The governing differential equations are solved numerically using MATLAB's bvp5c collocation method, which ensures high accuracy while overcoming the limitations of analytical techniques. This numerical framework enables a broad parametric investigation and delivers reliable predictions of flow characteristics. By adjusting key dimensionless parameters for both slip and no-slip cases, a systematic assessment is performed. The role of slip in influencing fluid motion and thermal transport is further underscored through a dedicated analysis of slip-only flow profiles. Under slip conditions, various intrinsic flow features affect the surface friction drag, convective heat transfer rate, and dimensionless mass transfer coefficient, all of which are thoroughly examined and presented through graphical illustrations.

2. MATHEMATICAL FORMULATION

We have conducted an investigation on the flow of a viscoelastic fluid across a deforming heated stretching sheet in a rotating frame of reference while adhering to a second-grade fluid model (Figure 1.), with a linear velocity of,

$$u_s(x) = ax, \tag{1}$$

where a represents a fixed constant, the plane expands in the x-direction while dwelling at z = 0. The fluid is subjected to an angular velocity rotating frame of reference [0, 0, Ω]. The surface temperature is determined by

$$T_s(x) = T_\infty + bx^2, \tag{2}$$

and the surface concentration is determined by

$$C_s(x) = C_\infty + b_1 x^2, \tag{3}$$

both of which are maintained under non-isothermal conditions. Here, T_∞ represents the ambient temperature, C_∞ denotes the ambient concentration, and b and b_1 are constants. The longitudinal, transverse and vertical velocity components are expressed as u, v, and w, respectively. Additionally, the influence of the Dufour effect is considered to capture the additional heat flux caused by concentration gradients together with multiple slips and moreover, the flow described by the governing equations are modified to incorporate the effects of Coriolis and centrifugal forces owing to rotation.

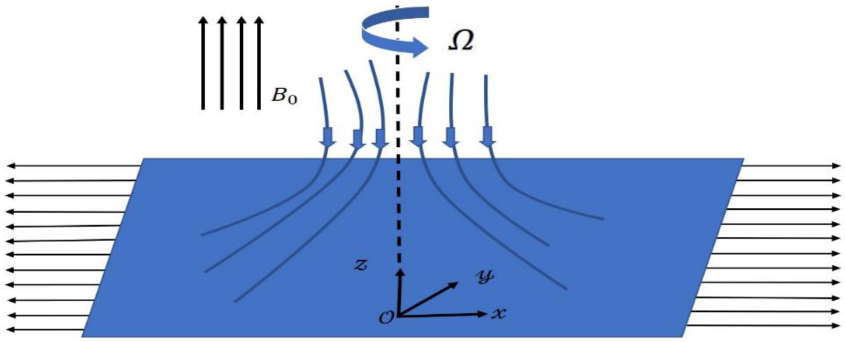

Figure 1. shows a fluid flow representation in a rotational frame of reference across a stretching surface.

Assuming laminar flow and fluid incompressibility, the following are the equations that governs the fluid flow.

$$\nabla \cdot \mathbf{V} = 0 \tag{4}$$

$$\rho\{(\mathbf{V} \cdot \nabla)\mathbf{V} + (2\Omega \times \mathbf{V}) + \Omega \times (\Omega \times \mathbf{r})\} = -\nabla \mathrm{p} + \nabla \cdot \boldsymbol{\mathcal{T}} + \mathbf{J} \times \mathbf{B} \tag{5}$$

$$\rho c_p\{(\mathbf{V} \cdot \nabla)\mathrm{T}\} = \kappa \nabla^2 \mathrm{T} + \boldsymbol{\mathcal{T}}: \nabla \mathbf{V} + \sigma B_0^2(\mathbf{V} \cdot \mathbf{V}) + \rho \frac{\mathrm{D} k_T}{c_s} \nabla^2 \mathrm{C} \tag{6}$$

$$(\mathbf{V} \cdot \nabla)\mathrm{C} = \mathrm{D}\nabla^2 \mathrm{C} + \frac{\mathrm{D} k_T}{T_m} \nabla^2 \mathrm{T} \tag{7}$$

where $\mathbf{B} = [0, 0, B_0]$ represents the magnetic force field vector, $\mathbf{V}$ is the fluid velocity, k_T denotes the coefficient of thermophoretic diffusion, T_m indicates the average fluid temperature, $\Omega = [0, 0, \Omega]$ is the rotational velocity vector, c_p is isobaric specific heat, c_s is saturated specific heat , D refers to the diffusivity coefficient for mass transfer, b_m shows the current density, and ρ is the volumetric mass density .

The stress tensor for second-grade fluid model is represented as follows:

$$\boldsymbol{\mathcal{T}} = -\mathrm{p}\mathbf{I} + \mu \mathbf{A_1} + \alpha_1 \mathbf{A}_2 + \alpha_2 \mathbf{A}_1^2 \tag{8}$$

where p denotes the thermodynamic pressure, α_1 is the elasticity modulus, **I** referred to as the unit tensor, μ is dynamic viscosity, $\boldsymbol{\mathcal{T}}$ is the stress tensor, and α_2 corresponds to the transverse viscosity parameter. Additionally, α_1 and α_2 together account for normal stress effects in the fluid system such that

$$\alpha_1 > 0 \quad \text{and} \quad \alpha_1 + \alpha_2 = 0 \tag{9}$$

The Rivlin-Ericksen tensors are expressed as:

$$\mathbf{A}_1 = (\nabla\mathbf{V}) + (\nabla\mathbf{V})^t \tag{10}$$

$$\mathbf{A}_2 = \left(\frac{d}{dt}\right)\mathbf{A}_1 + \mathbf{A}_1(\nabla\mathbf{V}) + (\nabla\mathbf{V})^t\mathbf{A}_1 \tag{11}$$

Following the boundary layer approximations, the resulting formulations were derived,

$$u_x + v_y + w_z = 0, \tag{12}$$

$$uu_x + vu_y + wu_z - 2\Omega v = \nu u_{zz} + \frac{\alpha_1}{\rho}(uu_{xzz} - u_z v_{zy} + vu_{yzz} + wu_{zzz} - u_z w_{zz} + u_x u_{zz} + v_x v_{zz} + v_z v_{xz}) - \frac{\sigma B_0^2 u}{\rho}, \tag{13}$$

$$uv_x + vv_y + wv_z + 2\Omega u = \nu v_{zz} + \frac{\alpha_1}{\rho}(uv_{xzz} - v_z u_{xz} + vv_{yzz} + wv_{zzz} - v_z w_{zz} + u_y u_{zz} + u_z u_{yz} + v_y v_{zz}) - \frac{\sigma B_0^2 v}{\rho}, \tag{14}$$

$$uT_x + vT_y + wT_z = \alpha T_{zz} + \frac{\alpha_1}{\rho c_p}(uu_{xz}u_z + vu_{zy}u_z + wu_{zz}u_z + uv_{xz}v_z + vv_{zy}v_z + wv_{zz}v_z) + \frac{\nu}{c_p}(u_z^2 + v_z^2) + \frac{\sigma B_0^2}{\rho c_p}(u^2 + v^2) + \frac{Dk_T}{c_p c_s}C_{zz}, \tag{15}$$

$$uC_x + vC_y + wC_z = DC_{zz} + \frac{Dk_T}{T_m}T_{zz}. \tag{16}$$

where, heat diffusion rate is represented by $\alpha = \frac{\kappa}{\rho c_p}$, while $\nu = \frac{\mu}{\rho}$ defines the momentum diffusivity ratio, conductivity of the fluid is denoted by σ, and magnetic flux density is indicated by B_0. Furthermore, α_1 symbolizes the fluid property coefficient associated with viscoelasticity.

Using the impermeable wall and the multiple slip assumption, boundary conditions are enforced as:

$$u(x,0) = u_s(x) = ax + \mu_f\frac{\partial u}{\partial z}, \;\; v(x,0) = 0, \;\; w(0) = 0, T = T_s(x) + \mu_t\frac{\partial T}{\partial z}, C = C_s(x) + \mu_c\frac{\partial C}{\partial z}. \tag{17}$$

$$u \to 0, u_z \to 0, v \to 0, v_z \to 0, T \to T_\infty, C \to C_\infty, \text{as } z \to \infty. \tag{18}$$

The similarity transformations are defined as follows:

$$u = axf'(\xi), v = axg(\xi), w = -\sqrt{a\nu}f(\xi), \theta(\xi) = \frac{T - T_\infty}{T_s - T_\infty}, \phi(\xi) = \frac{C - C_\infty}{C_s - C_\infty}. \tag{19}$$

where $\xi = z\sqrt{\frac{a}{\nu}}$ denotes similarity variable.

Non-dimensional equations obtained after the transformations are as follows:

$$f''' - f'^2 + ff'' + 2\lambda g + K(2f'f''' - ff'''' + f''^2 + gg'' + g'^2) - Mf' = 0 \tag{20}$$

$$g'' + fg' - f'g - 2\lambda f' + K(f'g'' - fg''') - Mg = 0 \tag{21}$$

$$\theta'' + Pr(f\theta' - 2f'\theta) + Pr\,Ec\,(f''^2 + g'^2 + K(f'f''^2 + f'g'^2 - f f'' f''' - f g' g'')) + Pr\,Ec\,M(f'^2 + g^2) + D_f\phi'' = 0 \tag{22}$$

$$\phi'' + Sc(f\phi' - 2f'\phi) + Sr\,\theta'' = 0 \tag{23}$$

where K denotes the elasticity coefficient, while λ signifies the rotational parameter. Ec refers to the Eckert number, and M represents the magnetic field parameter. Additionally, Pr highlights the Prandtl number, Sc describes the Schmidt number, Sr accounts for Soret effect parameter and, D_f represents the Dufour number are represented as follows:

$$K = \frac{\alpha_1 a}{\mu}, \lambda = \frac{\Omega}{a}, \; Ec = \frac{a^2}{bc_p}, \; M = \frac{\sigma B_0^2}{\rho a}, \; Pr = \frac{\nu}{\alpha}, \; Sc = \frac{\nu}{D}, \; Sr = \frac{k_T}{T_m}\left(\frac{T_s - T_\infty}{C_s - C_\infty}\right), D_f = \frac{Dk_T(C_s - C_\infty)}{c_p c_s \alpha (T_s - T_\infty)}. \tag{24}$$

The transformed boundary conditions are,

$$f = 0, \quad g = 0, \quad f' = 1 + \gamma f'', \quad \theta = 1 + \alpha\theta', \quad \phi = 1 + \beta\phi' \quad \text{at} \quad \xi = 0. \tag{25}$$

$$f' \to 0, \quad f'' \to 0, \quad g \to 0, \quad g' \to 0, \quad \theta \to 0, \quad \phi \to 0 \quad \text{as} \quad \xi \to \infty. \tag{26}$$

where $\gamma, \alpha,$ and β represent the momentum slip coefficient, heat slip coefficient, and mass slip coefficient, respectively.

To investigate the drag experienced at the surface of the plate $z = 0$, the wall shear stress coefficients in the x- and y-directions, along with the dimensionless heat and mass transfer numbers, are defined as follows:

$$C_{fx} = \frac{\mathcal{T}_{zx}|_{z=0}}{\rho u_s^2}, C_{fy} = \frac{\mathcal{T}_{zy}|_{z=0}}{\rho u_w^2}, Nu_x = \frac{xq_w}{k(T_w - T_\infty)}, Sh_x = \frac{xj_w}{D(C_w - C_\infty)}. \tag{27}$$

where the coefficients of friction along $x-$ and $y-$ axes are denoted as C_{fx} and C_{fy}, respectively. $\mathcal{T}_{zx}$ and $\mathcal{T}_{zy}$ represent the shear stresses at $z = 0$. ρ is the fluid density, u represents velocity scale (possibly free-stream velocity), $q_w = -k\left(\frac{\partial T}{\partial z}\right)_{z=0}$ signifies the thermal flux through the wall and $j_w = -D\left(\frac{\partial C}{\partial z}\right)_{z=0}$ gives a mass flux through the wall.

The shear stress is represented as follows,

$$\mathcal{T}_{zx} = \mu u_z + \alpha_1\left(uu_{xz} - u_z w_z + vu_{yz} + wu_{zz} + u_x u_z + v_x v_z\right), \tag{28}$$

$$\mathcal{T}_{zy} = \mu v_z + \alpha_1\left(uv_{xz} - v_z w_z + vv_{zy} + wv_{zz} + u_y u_z + v_y v_z\right), \tag{29}$$

The transformed equations are obtained using Eq. (19) are as follows,

$$C_{fx}Re_x^{1/2} = (1 + 3K)f''(0), \tag{30}$$

$$C_{fy}Re_x^{1/2} = (1 + 2K)g'(0), \tag{31}$$

$$N_{u_x}Re_x^{1/2} = -\theta'(0), \tag{32}$$

$$S_{h_x} Re_x^{1/2} = -\phi'(0). \quad (33)$$

where $Re_x = \frac{u_s x}{\nu}$ describes the spatial Reynolds number. Both the position-dependent Nusselt number and the Sherwood number vary in proportion to $\theta'(0)$ and $\phi'(0)$, respectively.

3. NUMERICAL METHODOLOGY

The resulting equation (20)-(23), along with the boundary conditions (25) and (26), has been evaluated numerically by the use of MATLAB's bvp5c solver and the collocation method. The first step in obtaining a numerical solution with bvp5c is to reformulate the equations into a system of first-order equations using the appropriate substitutions listed below.

$$f = Y_1,\ f' = Y_2,\ f'' = Y_3, f''' = Y_4,\ g = Y_5,\ g' = Y_6,\ g'' = Y_7,\ \theta = Y_8,\ \theta' = Y_9,\ \phi = Y_{10},\ \phi' = Y_{11}. \quad (34)$$

Substituting Eq. (34) in Eq. (20)-(23), we get modified equations as listed below,

$$Y_4' = \frac{\left(K\left(2Y_2Y_4 + Y_3^2 + Y_5Y_7 + Y_6^2\right) + Y_4 - Y_2^2 + Y_1Y_3 + 2\lambda Y_5 - MY_2\right)}{KY_1}, \quad (35)$$

$$Y_7' = \frac{KY_2Y_7 + Y_7 + Y_1Y_6 - Y_2Y_5 + 2\lambda Y_2 - MY_5}{KY_1}, \quad (36)$$

$$Y_9' = -Pr(Y_1Y_9 - 2Y_2Y_8) - \ Pr\ Ec\ (Y_3^2 + Y_6^2\ ) - Pr\ Ec\ K\ (Y_2Y_3^2 + Y_2Y_6^2 - Y_1Y_3Y_4 - Y_1Y_6Y_7) - Pr\ Ec\ M(Y_2^2 + Y_5^2)\ - D_f Y_{11}', \quad (37)$$

$$Y_{11}' = -Sc(Y_1Y_{11} - 2Y_2Y_{10}) - SrY_9'. \quad (38)$$

and similarly, the boundary conditions Eq. (25) and Eq. (26) takes the form,

$$Y(0) = 0, \quad Y_2(0) = 1 + \gamma Y_3, \quad Y_5(0) = 0, \quad Y_8(0) = 1 + \alpha Y_9, \quad Y_{10}(0) = 1 + \beta Y_{11}. \quad (39)$$

$$Y_2(+\infty) = 0,\ Y_3(+\infty) = 0,\ Y_5(+\infty) = 0, Y_6(+\infty) = 0, Y_8(+\infty) = 0, Y_{10}(+\infty) = 0. \quad (40)$$

The bvp5c approach precisely integrates the previously specified system of equations using a finite difference algorithm based on a collocation formula that utilized an implicit Runge-Kutta approach. The criteria at infinity are met here with the specified tolerance of 10^{-4}.

4. RESULTS AND DISCUSSION

This section examines the effects of various governing parameters, including K, λ, M, D_f, Sc, and Sr on the velocity, temperature, and concentration profiles of a viscoelastic fluid flow over a heated flat surface in a rotating frame, considering both slip and no-slip conditions. These parameters are assigned specific ranges based on prior fluid flow studies and well-established assumptions. In particular, $0 \leq K \leq 2$, $0 \leq \lambda \leq 1.5$, $0 \leq M \leq 2$, $0 \leq D_f \leq 1.5$, $1 \leq Sc \leq 2$, and $0 \leq Sr \leq 1$. Additionally, the multiple slip parameters have the following ranges: $0 \leq \gamma \leq 1$, $0 \leq \alpha \leq 0.2$, and $0 \leq \beta \leq 0.2$.

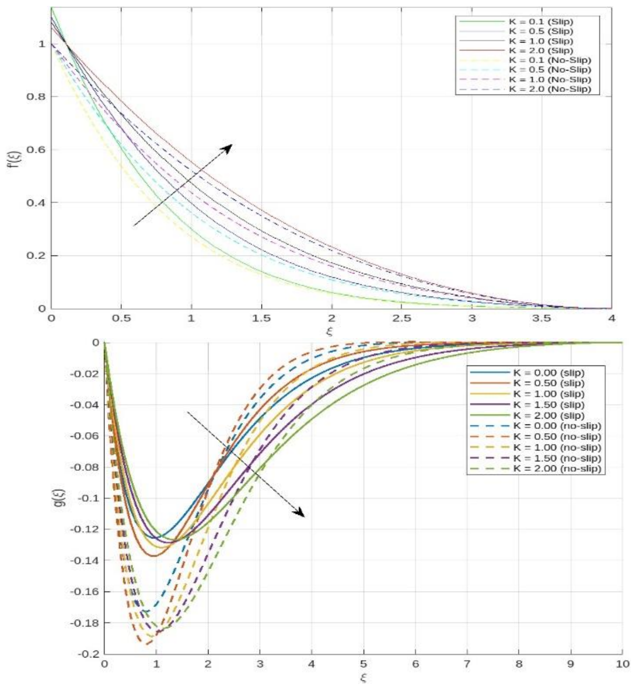

Figure 2(i) **Figure 2(ii)**

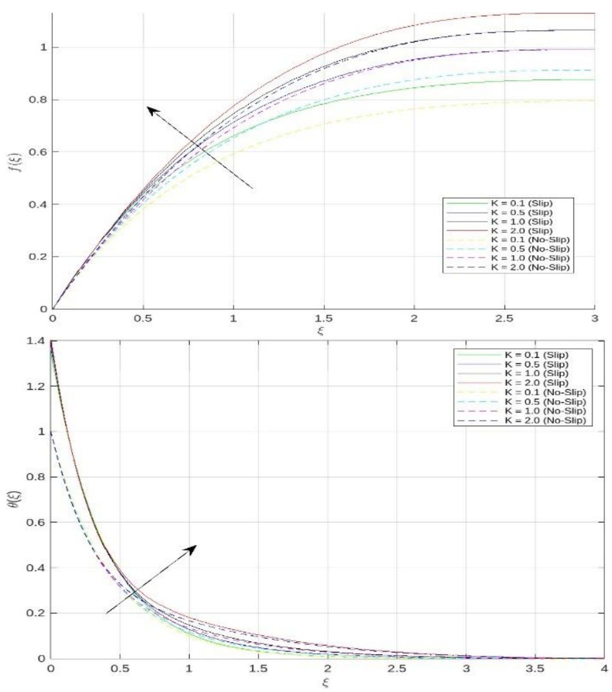

Figure 2(iii) **Figure 2(iv)**

Figure 2(i)–2(iv). demonstrates the velocity profiles $f'(\xi), g(\xi), f(\xi)$,and thermal profile $\theta(\xi)$ for different values of the elastic modulus parameter (K).

Normal stress and elasticity are represented by the elastic parameter K in second grade fluid. In Fig. 2(i) and Fig. 2(iii), increasing K causes the fluid to stretch more efficiently in the primary direction and decrease resistance to deformation, which increases longitudinal velocity. The slip condition further improves the velocity profile by lowering friction at the surface. Elasticity improves streamline alignment with the stretching direction, limiting transverse (cross-flow) motion Fig.

2(ii). As seen in Fig. 2(iv), temperature decreases near the wall because heat is initially convected more effectively as the elasticity parameter rises, and it increases farther from the wall as the convective effect lessens, resulting in temperature accumulation.

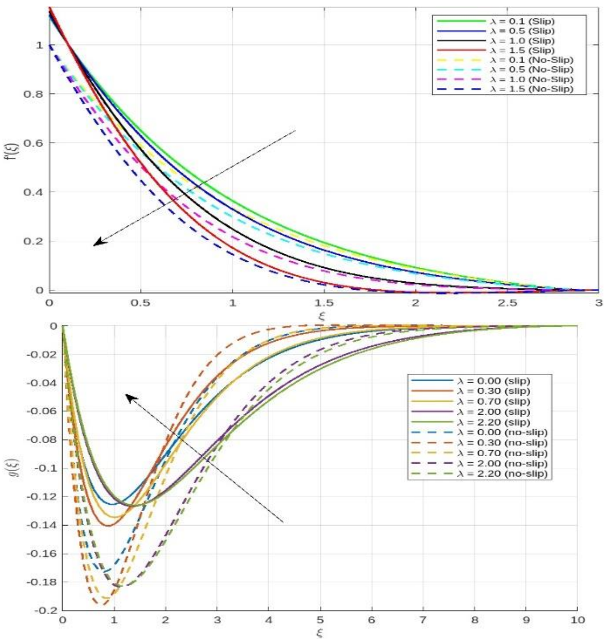

Figure 3(i) **Figure 3(ii)**

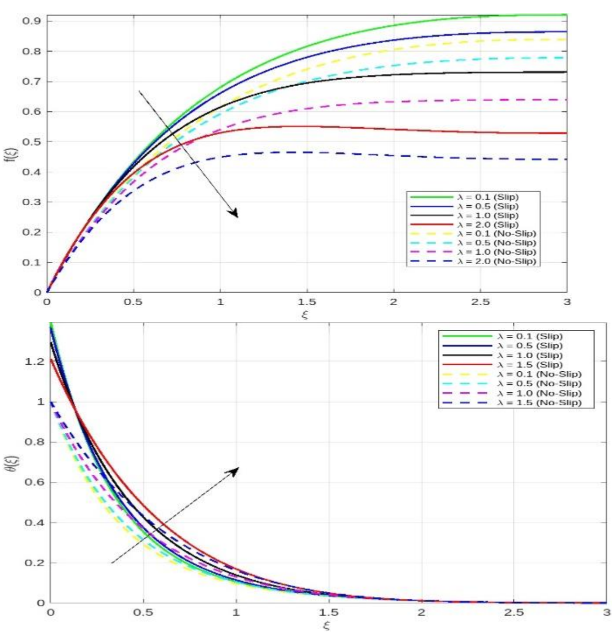

Figure 3(iii) **Figure 3(iv)**

Figure 3(i)–3(iv). demonstrates the velocity profiles $f'(\xi), g(\xi), f(\xi)$,and thermal profile $\theta(\xi)$ for different values of the rotation parameter (λ).

Rotation in a Newtonian fluid mostly causes the flow to be redirected. However, as seen in Fig. 3(i) and Fig. 3(iii), elasticity moderates rotation to some degree, but at larger rotational values, it exceeds the viscoelastic effect, which suppresses primary velocities. Second-grade fluids have stronger vertical velocities than Newtonian fluids because of the way the rotation redistributes momentum due to normal stress differences, as shown in Fig. 3(ii). Additionally, Fig. 3(iv), illustrates that rotation decreases momentum transfer, which hinders convective heat transport and causes heat accumulation.

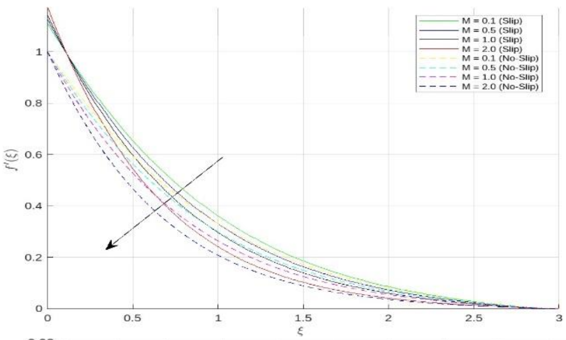

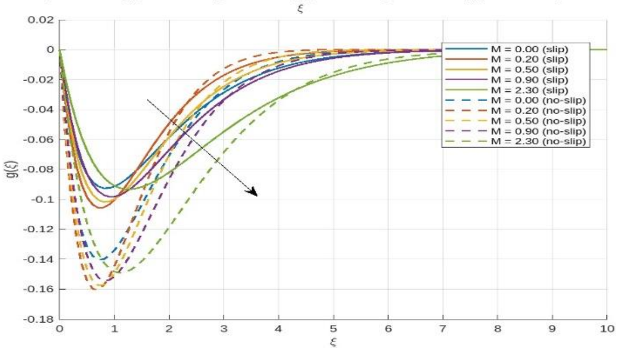

Figure 4(i) **Figure 4(ii)**

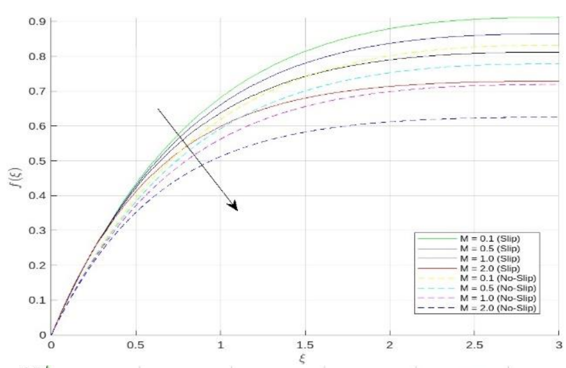

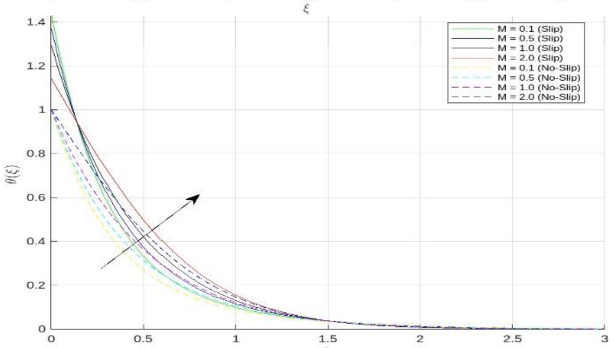

Figure 4(iii) **Figure 4(iv)**

Figure 4(i)–4(iv). demonstrates the velocity profiles $f'(\xi), g(\xi), f(\xi)$, and thermal profile $\theta(\xi)$ for different values of the magnetic field strength $(\mathbf{M})$.

The Lorentz force functions as a counteracting force, damping velocity even when rotated. Regardless of whether slippage occurs at the wall or not, the magnetic field nevertheless dampens the flow in the bulk zone. Fig. 4(i)–Fig. 4(iii), demonstrate how momentum stretching is prevented in both scenarios, resulting in consistent velocity suppression. Joule heating occurs when the fluid's electrical resistance retards convective motion heat transmission and elevates its temperature Fig. 4(iv).

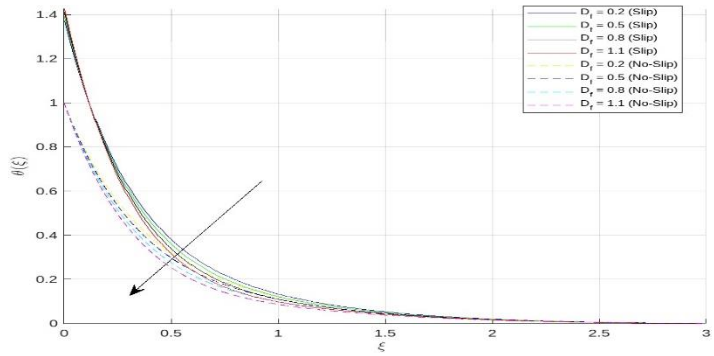

Figure 5. shows the temperature field for different variations of Dufour number.

The phenomenon known as the "Dufour effect" occurs when a mixture's concentration gradient generates a heat flux that results in localized heating. Fig. 5, shows the effect of the Dufour number, and it is discovered that when the heat distribution drops, mass diffusion causes the system to cool. In the absence of slip conditions, heat is transferred by conduction and diffusion; with slip flow conditions, however, convective thermal transfer takes place, enabling further energy transfer out of the system to improve cooling.

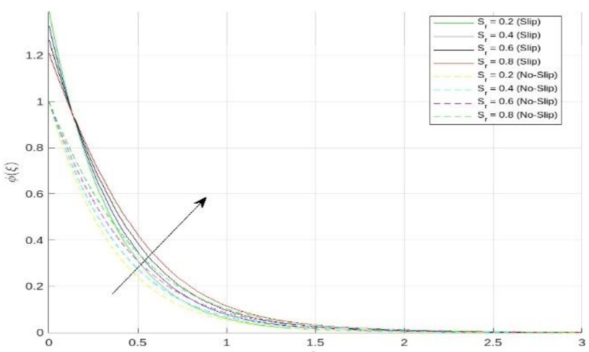

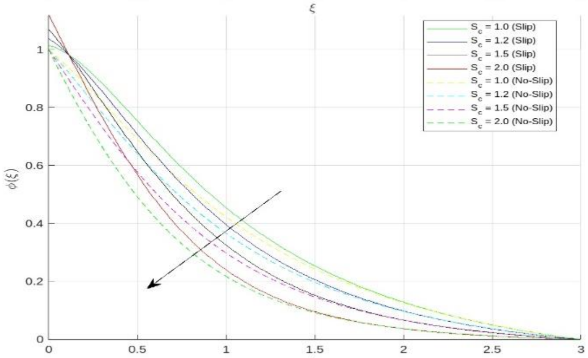

Figure 6(i) **Figure 6(ii)**

Figure 6(i)–6(ii). demonstrates the concentration distribution across various values of Soret number and Schmidt number.

Species migration from hot to cold areas is caused by a temperature gradient. Fig. 6(i), shows how slip weakens the layer, increasing mass diffusion. Fig. 6(ii), illustrates the Schmidt number effect on concentration. Higher Sc results in greater concentrations near the surface, but slip conditions facilitate species migration, reducing surface concentration. Compared to no-slip, the concentration boundary layer is thinner.

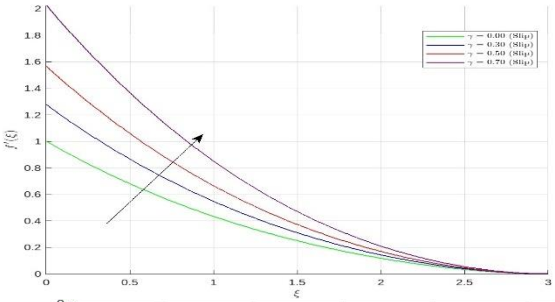

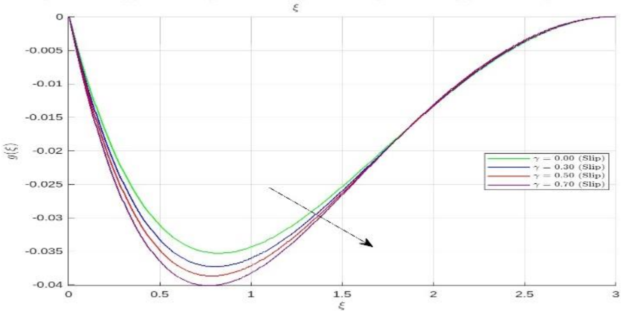

Figure 7(i) **Figure 7(ii)**

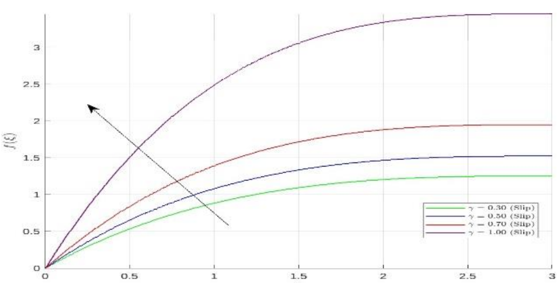

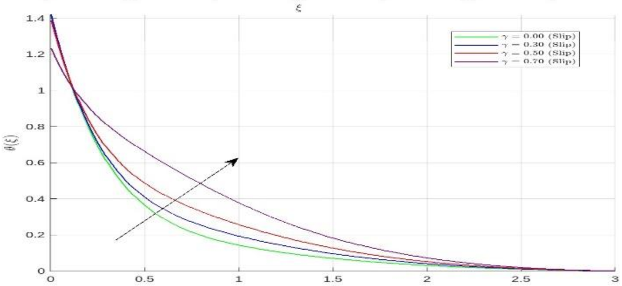

Figure 7(iii) **Figure 7(iv)**

Figure 7(i)–7(iv). demonstrates the velocity profiles $f'(\xi), g(\xi), f(\xi)$,and thermal profile $\theta(\xi)$ for different velocity slips (γ).

In Fig.7(i)– Fig. 7(iv), elevated slip values generally enhance the fluid velocity, thereby lowering the shear stress at the boundary and facilitating momentum transfer. Additionally, it builds up the thermal state of the fluid by reducing the thermal boundary layer depth, which also leads to more efficient heat transfer.

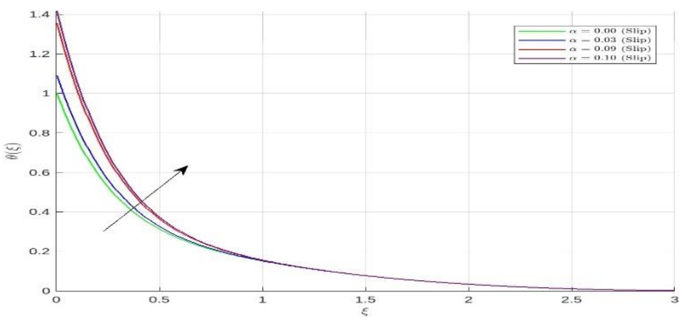

Figure 8. demonstrates the impact of heat slip on fluid thermal distribution.

In Fig. 8, thermal slip has been found to raise fluid temperature. It enhances convective heat transmission and lowers thermal resistance.

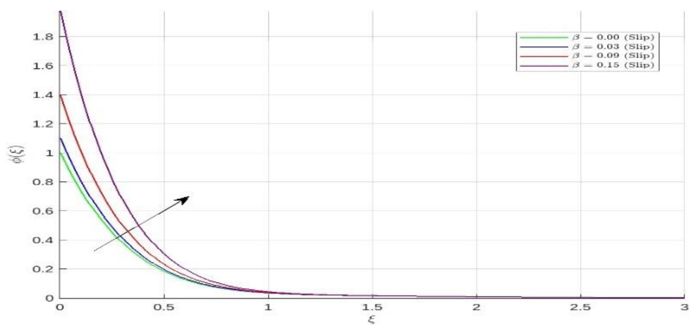

Figure 9. demonstrates the effect of concentration Slip on Mass Diffusion.

In Fig. 9, as the concentration slip increases, the concentration boundary layer thins, increasing the mass diffusion rate. Additionally, the impact influences interactions between molecules at the surface and stimulates mass transfer and chemical processes.

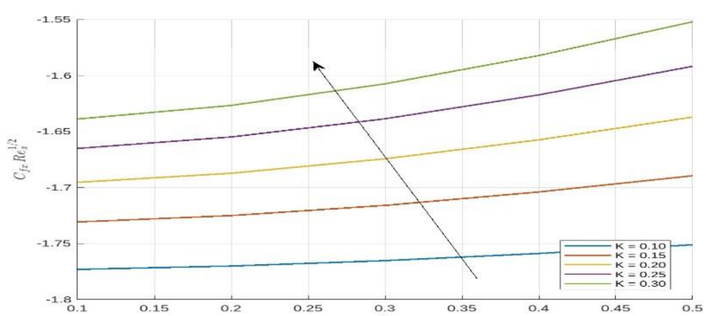

Figure 10. demonstrates the role of the elasticity factor (K) in determining surface friction under the influence of rotation.

In Fig. 10, notably, secondary flows are induced by Coriolis forces, which improve momentum transmission. Increasing the elasticity parameter K increases the resistance to motion at the surface; as a result, the combined effect of elasticity and rotation raises the surface velocity gradient and, consequently, skin friction. In thermal systems, higher skin friction frequently corresponds to higher heat transfer rates.

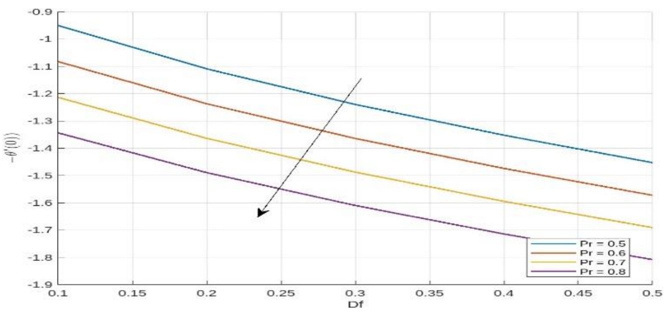

Figure 11. demonstrates the effect of Dufour number (Df)on the heat transfer efficiency for different Prandtl number (Pr) values.

In Fig. 11, heat transmission efficiency is reduced when momentum diffusion predominates over thermal diffusion (high Pr). Convective heat transmission is weakened as a result.

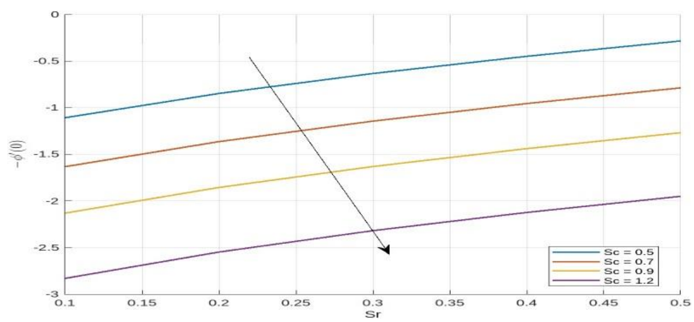

Figure 12. demonstrates the impact of Schmidt number (Sc) under the influence of Soret number (Sr) on the Sherwood number.

In Fig. 12, the graph depicts the Sherwood number in relation to various Schmidt and Soret numbers. It shows that decreasing the Schmidt number facilitates mass diffusion, while an increase leads to its reduction. Additionally, the Soret effect plays a role in mass redistribution, which mitigates the convective concentration gradient at the boundary and ultimately results in decreased mass transfer.

5. CONCLUSION

This paper investigates the movement of a second-grade fluid in a revolving frame across a deforming sheet taking into account various slip circumstances as well as the impact of the Soret and Dufour phenomena. Utilizing the collocation technique built into MATLAB's bvp5c solver, the analysis is carried out. Multiple slips and the Dufour effect are the novel factors in this study. The key findings of the present investigation are listed below.

- Elasticity improves streamlined alignment, restricting transverse motion, and initially increasing convective heat transmission near the wall, resulting in temperature accumulation further away.
- The Lorentz force, regardless of wall slip, dampens velocity and prevents momentum stretching. Joule heating raises fluid temperature by slowing convective heat transport.
- The greater the Coriolis force intensity or rotation rate, the fluid is inhibited longitudinally, resulting in a thicker boundary layer with greater cross flow effects. It also causes temperature accumulation away from the wall since heat is transported transversely.
- The interaction of Dufour and Soret effects with viscoelasticity alters thermal boundary layer thickness, influencing heat transport efficiency.
- Higher slip values increase velocity while minimizing shear stress and enhancing

momentum transfer. This also thins the thermal boundary layer, raising fluid temperatures and increasing heat transfer efficiency.

- Thermal slip raises fluid temperature, enhancing convective heat transfer and reducing thermal resistance.
- Increasing concentration slip thins the concentration boundary layer, enhancing the mass diffusion rate.
- Higher skin friction often increases heat transfer rates but weakens convective heat transmission. The Soret effect redistributes mass, reducing the convective concentration gradient and lowering mass transfer.

This research provides critical insights into the combined effects of viscoelasticity, electromagnetic forces, rotation, and slip conditions on fluid flow, heat, and mass transfer. By uncovering how these factors influence boundary layer behavior and transport efficiency, the study offers a foundation for optimizing complex fluid systems. Its applications span microfluidic devices, magnetohydrodynamic cooling systems, rotating machinery, chemical reactors, and biomedical technologies, where precise control of thermal and mass transport is essential for performance and innovation.

REFERENCES

[1] A. Lavrov, "Flow of Non-Newtonian Fluids in Single Fractures and Fracture Networks: Current Status, Challenges, and Knowledge Gaps", Engineering Geology, vol. 321, **(2023)**, pp. 107166.

[2] M.I. Khan and F. Alzahrani, "Numerical Simulation for the Mixed Convective Flow of Non-Newtonian Fluid with Activation Energy and Entropy Generation", Case Studies in Thermal Engineering, vol. 45, **(2023)**, pp. 103035.

[3] K.A.M. Alharbi, A. Ullah, I. Nahid, F. Ali, R. Khan and S. Khan, "Impact of Viscous Dissipation and Coriolis Effects in Heat and Mass Transfer Analysis of the 3D Non-Newtonian Fluid Flow", Case Studies in Thermal Engineering, vol. 37, **(2022)**, pp. 102289.

[4] A. Hammer, W. Roland, C. Marschik and G. Steinbichler, "Predicting the Co-extrusion Flow of Non-Newtonian Fluids Through Rectangular Ducts – A Hybrid Modeling Approach", Journal of Non-Newtonian Fluid Mechanics, vol. 295, **(2021)**, pp. 104618.

[5] R. Hashim, S. Rehman, E.M. Tag Eldin, O.T. Bafakeeh and K. Guedri, "Coupled Energy and Mass Transport for Non-Newtonian Nanofluid Flow Through Non-parallel Vertical Enclosure", Ain Shams Engineering Journal, vol. 14, **(2023)**, pp. 102023.

[6] K.U. Rehman and W. Shatanawi, "Non-Newtonian Mixed Convection Magnetized Flow with Heat Generation and Viscous Dissipation Effects: A Prediction Application of Artificial Intelligence", Processes, vol. 11, **(2023)**, pp. 986.

[7] A. Ali, M. Awais, A. Al-Zubaidi, S. Saleem and D.N. Khan Marwat, "Hartmann Boundary Layer in Peristaltic Flow for Viscoelastic Fluid: Existence", Ain Shams Engineering Journal, vol. 13, **(2022)**, pp. 101555.

[8] H. Vaidya, K.V. Prasad, M. Gudekote, D. Tripathi, R. Choudhari and H. Hanumantha, "A Comprehensive Analysis of Magnetized Non-Newtonian Nanofluids' Peristaltic Mechanism for Optimized Fluid Flow and Heat Transfer", Case Studies in Thermal Engineering, vol. 61, **(2024)**, pp. 104929.

[9] M. Akram, et al., "Exploring the Dynamic Behavior of the Two-phase Model in Radiative Non-Newtonian Nanofluid Flow with Hall Current and Ion Slip Effects", Journal of Radiation Research and Applied Sciences, vol. 17, **(2024)**, pp. 101112.

[10] S. Fakhar, M. Mustafa and T. Ibrahim, "Exploring Entropy Production in MHD Walters-B Fluid Motion in a Rotating Frame with Frictional Heating Using OHAM-Based Package BVPh 2.0", International Journal of Hydrogen Energy, vol. 90, **(2024)**, pp. 1252-1262.

[11] S. Bilal, A.H. Majeed, R. Mahmood, I. Khan, A.H. Seikh and E.-S.M. Sherif, "Heat and Mass Transfer in Hydromagnetic Second-Grade Fluid Past a Porous Inclined Cylinder under the Effects of Thermal Dissipation, Diffusion and Radiative Heat Flux", Energies, vol. 13, **(2020)**, pp. 278.

[12] Kh. Hosseinzadeh, et al., "Investigation of Second-Grade Viscoelastic Non-Newtonian Nanofluid Flow on the Curve Stretching Surface in Presence of MHD", Results in Engineering, vol. 17, **(2023)**, pp. 100838.

[13] N. Mustafa, S. Asghar and M.A. Hossain, "Natural Convection Flow of Second-Grade Fluid Along a Vertical Heated Surface with Variable Heat Flux", International Journal of Heat and Mass Transfer, vol. 53, **(2010)**, pp. 5856-5862.

[14] K. Vajravelu, "Viscous Flow over a Nonlinearly Stretching Sheet", Applied Mathematics and Computation, vol. 124, **(2001)**, pp. 281-288.

[15] M. Alrehili, "Viscoelastic Thermal Nanofluid Flow and Heat Mass Transfer Due to a Stretching Sheet with Slip Velocity Phenomenon and Convective Heating", International Journal of Thermofluids, vol. 17, **(2023)**, pp. 100281.

[16] M.R. Eid and F. Mabood, "Thermal Analysis of Higher-Order Chemical Reactive Viscoelastic Nanofluids Flow in Porous Media via Stretching Surface", Proceedings of the Institution of Mechanical Engineers, Part C: Journal of Mechanical Engineering Science, vol. 235, **(2021)**, pp. 6099-6110.

[17] S.I. Abdelsalam, W. Abbas, A.M. Megahed and A.A.M. Said, "A Comparative Study on the Rheological Properties of Upper Convected Maxwell Fluid Along a Permeable Stretched Sheet", Heliyon, vol. 9, **(2023)**, e22740.

[18] S. Rehman, N. Muhammad, M. Alshehri, S. Alkarni, S.M. Eldin and N.A. Shah, "Analysis of a Viscoelastic Fluid Flow with Cattaneo–Christov Heat Flux and Soret–Dufour Effects", Case Studies in Thermal Engineering, vol. 49, **(2023)**, pp. 103223.

[19] S. Zeb, Z. Ullah, H. Urooj, I. Khan, A.H. Ganie and S.M. Eldin, "Simultaneous Features of MHD and Radiation Effects on the UCM Viscoelastic Fluid Through a Porous Medium with Slip Conditions", Case Studies in Thermal Engineering, vol. 45, **(2023)**, pp. 102847.

[20] M. Bilal, S. Khan, F. Ali, M. Arif, I. Khan and K.S. Nisar, "Couette Flow of Viscoelastic Dusty Fluid in a Rotating Frame Along with the Heat Transfer", International Journal of Thermofluids, vol. 22, **(2022).**

[21] D. Khan, V. Kumam, A.U. Rahman, G. Ali, K. Sitthithakerngkiet, W. Watthayu and A.M. Galal, "The Outcome of Newtonian Heating on Couette Flow of Viscoelastic Dusty Fluid Along with the Heat Transfer in a Rotating Frame: Second Law Analysis", Heliyon, vol. 8, **(2022)**, e10538.

[22] S.S. Akbar and M. Mustafa, "Coupled Heat and Mass Transfer to Viscoelastic Fluid Flow in a Rotating Frame Using Series and Numerical Solutions", International Journal of Heat and Fluid Flow, vol. 106, **(2024)**, pp. 109294.

[23] T. Hayat, R. Naz, S. Asghar and A. Alsaedi, "Soret-Dufour Effects on MHD Rotating Flow of a Viscoelastic Fluid", International Journal of Numerical Methods for Heat and Fluid Flow, vol. 24, **(2014)**, pp. 498-520.

[24] H. Mondal, D. Pal, S. Chatterjee and P. Sibanda, "Thermophoresis and Soret-Dufour on MHD Mixed Convection Mass Transfer Over an Inclined Plate with Non-uniform Heat Source/Sink and Chemical Reaction", Ain Shams Engineering Journal, vol. 9, **(2018)**, pp. 2111-2121.

[25] M.M. Rashidi, M. Ali, B. Rostami, P. Rostami and G.N. Xie, "Heat and Mass Transfer for MHD Viscoelastic Fluid Flow Over a Vertical Stretching Sheet with Considering Soret and Dufour Effects", **(2015)**.

[26] Md. Hasanuzzaman, M.M.H. Milon, M.M. Hossain and Md. Asaduzzaman, "Dufour and Thermal Diffusion Effects on Time-Dependent Natural MHD Convective Transport Over an Inclined Porous Plate", International Journal of Thermofluids, vol. 21, **(2024)**, pp. 100572.

[27] M. Harikrushna, G. Prabhakara Rao and M. Veera Krishna, "Soret and Dufour Effects on the Magnetohydrodynamic Free Convective Flow of Maxwell Nanofluid Past an Infinite Stretching Sheet", Proceedings of the Institution of Mechanical Engineers, Part E: Journal of Process Mechanical Engineering, **(2023)**.

[28] A. Ahmed, M. Khan, A. Zafar, M. Yasir and M. Ayub, "Analysis of Soret-Dufour Theory for Energy Transport in Bioconvective Flow of Maxwell Fluid", Ain Shams Engineering Journal, vol. 14, **(2023)**, pp. 102045.

[29] K. Sudarmozhi and D. Iranian, "Viscoelastic Fluid Flow on Channel in Porous Medium with Soret and Dufour Along with the Effect of Activation Energy and Suction and Blowing", Journal of Taibah University for Science, vol. 18, **(2024)**, pp. 2328869.

[30] G. Sreedevi, D.R.V. Rao, O.D. Makinde and G. Reddy, "Soret and Dufour Effects on MHD Flow with Heat and Mass Transfer Past a Permeable Stretching Sheet in Presence of Thermal Radiation", NISCAIR-CSIR, **(2017)**.

[31] Md. Hasanuzzaman, M.A. Labony and M.M. Hossain, "Heat Generation and Radiative Effects on Time-Dependent Free MHD Convective Transport Over a Vertical Permeable Sheet", Heliyon, vol. 9, **(2023)**, e20865.

[32] A.K. Gautam, S. Rajput, K. Bhattacharyya, A.K. Pandey, A.J. Chamkha and M. Begum, "Comparative Study of Two Non-Newtonian Fluids with Bioconvective Induced MHD Flow in Presence of Multiple Slips, Heat Source/Sink and Nonlinear Thermal Radiation", Chemical Engineering Journal Advances, vol. 12, **(2022)**, pp. 100365.

[33] N. Abbas, M. Ali, K.A. Abodayeh, Z. Mustafa and W. Shatanawi, "Thermal Investigation of Jeffrey Fluid Flow Past a Stretching Riga Curved Surface Under Soret and Dufour Impacts", Case Studies in Thermal Engineering, vol. 52, **(2023)**, pp. 103553.

[34] A.J. Chamkha and A.M. Rashad, "Unsteady Heat and Mass Transfer by MHD Mixed Convection Flow from a Rotating Vertical Cone with Chemical Reaction and Soret and Dufour Effects", Canadian Journal of Chemical Engineering, vol. 92, **(2014)**, pp. 758-767.

[35] F. Asmat, W.A. Khan, M.D. Shamshuddin, S.O. Salawu and M. Bouye, "Thermal Analysis in an Electrically Conducting Fluid with Multiple Slips and Radiation Along a Plate: A Case Study of Stokes' Second Problem", Case Studies in Thermal Engineering, vol. 44, **(2023)**, pp. 102831.

*[36] K. Sudarmozhi, D. Iranian, M.A. Memon, P.D. Selvi, M.S. Khan and A. Fenta, "Viscoelastic Fluid Flow Over a Horizontal Flat Plate with Various Boundary Slip Conditions and Suction Effects", Nanoscale Advances, vol. 5, **(2023)**, pp. 6102-6114.*